Spatiotemporal Properties of Fast and Slow Neurons in the Pretectal Nucleus Lentiformis Mesencephali in Pigeons

DOUGLAS R. W. WYLIE[1,2] AND NATHAN A. CROWDER[2]
[1]*Department of Psychology and* [2]*Division of Neuroscience, University of Alberta, Edmonton, Alberta T6G 2E9, Canada*

Received 4 April 2000; accepted in final form 8 August 2000

Wylie, Douglas R. W. and Nathan A. Crowder. Spatiotemporal properties of fast and slow neurons in the pretectal nucleus lentiformis mesencephali in pigeons. *J Neurophysiol* 84: 2529–2540, 2000. Neurons in the pretectal nucleus lentiformis mesencephali (LM) are involved in the analysis of optic flow that results from self-motion. Previous studies have shown that LM neurons have large receptive fields in the contralateral eye, are excited in response to largefield stimuli moving in a particular (preferred) direction, and are inhibited in response to motion in the opposite (anti-preferred) direction. We investigated the responses of LM neurons to sine wave gratings of varying spatial and temporal frequency drifting in the preferred and anti-preferred directions. The LM neurons fell into two categories. "Fast" neurons were maximally excited by gratings of low spatial [0.03–0.25 cycles/° (cpd)] and mid-high temporal frequencies (0.5–16 Hz). "Slow" neurons were maximally excited by gratings of high spatial (0.35–2 cpd) and low-mid temporal frequencies (0.125–2 Hz). Of the slow neurons, all but one preferred forward (temporal to nasal) motion. The fast group included neurons that preferred forward, backward, upward, and downward motion. For most cells (81%), the spatial and temporal frequency that elicited maximal excitation to motion in the preferred direction did not coincide with the spatial and temporal frequency that elicited maximal inhibition to gratings moving in the anti-preferred direction. With respect to motion in the anti-preferred direction, a substantial proportion of the LM neurons (32%) showed bi-directional responses. That is, the spatiotemporal plots contained domains of excitation in addition to the region of inhibition. Neurons tuned to stimulus velocity across different spatial frequency were rare (5%), but some neurons (39%) were tuned to temporal frequency. These results are discussed in relation to previous studies of the responses of neurons in the accessory optic system and pretectum to drifting gratings and other largefield stimuli.

INTRODUCTION

The pretectal nucleus lentiformis mesencephali (LM) is a retinal-recipient structure that is implicated in the processing of visual information resulting from self-motion ["optic flow" or "flowfields" (Gibson 1954)]. The LM and nuclei in the accessory optic system (AOS) are principally involved in the generation of visual optomotor responses including optokinetic nystagmus (OKN) and the opto-collic reflex (OCR) to facilitate retinal image stabilization (birds; Fite et al. 1979; Gioanni et al. 1983a,b; for reviews, see Grasse and Cynader 1990; Simpson 1984; Simpson et al. 1988). The LM is homologous to the nucleus of the optic tract (NOT) in mammals (Simpson et al. 1988). In numerous species, it has been shown that neurons in the LM and NOT exhibit direction selectivity in response to moving largefield stimuli that are rich in visual texture (i.e., random dot patterns or checkerboards). Although broadly tuned, most neurons are maximally excited in response to motion in the "preferred" direction and strongly inhibited in response to motion in the (approximately) opposite ("anti-preferred") direction (mammals: Collewijn 1975a,b; Hoffmann and Distler 1989; Hoffman and Schoppmann 1975, 1981; Hoffmann et al. 1988; Ibbotson et al. 1994; Mustari and Fuchs 1990; Volchan et al. 1989; birds: Fu et al. 1998a,b; Winterson and Brauth 1985; Wylie and Frost 1996; amphibians: Fan et al. 1995; Fite et al. 1989; Katte and Hoffmann 1980; Li et al. 1996; Manteuffel 1984).

Almost all of the preceding studies noted velocity tuning of LM and NOT in response to largefield stimuli consisting of random dot patterns, square-wave gratings, and/or checkerboards. However, Ibbotson et al. (1994), in a study of the wallaby NOT, used drifting sine wave gratings of varying spatial and temporal frequency (SF, TF) and suggested that cells were tuned to TF rather than velocity. They described two types of cells. "Slow" cells responded best to low TFs (<1 Hz) and high SFs [0.5–1 cycles/° (cpd)]. "Fast" cells were most responsive to high TFs (>10 Hz) and lower SFs (0.1–0.5 cpd) but had a secondary peak at low TFs and high SFs. In the present study, we recorded from neurons in the LM of pigeons in response to drifting sine wave gratings moving in the preferred and anti-preferred directions. This study permits a comparison of the spatiotemporal properties of pretectal neurons in differing species. Moreover, Wolf-Oberhollenzer and Kirschfeld (1994) have recorded the responses of neurons in the nucleus of the basal optic root (nBOR) of the AOS in pigeons to drifting sine wave gratings. Thus the present study also affords a comparison of the spatiotemporal properties of AOS and pretectal neurons in the same species. We have several previously unreported features to note.

METHODS

The methods reported herein conformed to the guidelines established by the Canadian Council on Animal Care and were approved by the Biosciences Animal Care and Policy Committee at the University of Alberta. Silver King and homing pigeons (obtained from a local supplier) were anesthetized with an intramuscular ketamine (65 mg/

Address for reprint requests: D.R.W. Wylie, Dept. of Psychology, University of Alberta, Edmonton, Alberta T6G 2E9, Canada (E-mail: dwylie@ualberta.ca).

The costs of publication of this article were defrayed in part by the payment of page charges. The article must therefore be hereby marked "*advertisement*" in accordance with 18 U.S.C. Section 1734 solely to indicate this fact.

kg)-xylazine (8 mg/kg) mixture. Depth of anesthesia was monitored periodically with a toe pinch, and supplemental doses were administered as necessary. The animals were placed in a stereotaxic device with pigeon ear bars and beak adapter so that the orientation of the skull conformed to the atlas of Karten and Hodos (1967). Based on the stereotaxic coordinates of Karten and Hodos (1967), sufficient bone and dura were removed to expose the brain and allow access the LM with a vertical penetration. Recordings were made with either tungsten microelectrodes (Frederick Haer) or glass micropipettes filled with 2 M NaCl and having tip diameters of 4–5 μm. The extracellular signal was amplified, filtered, displayed on an oscilloscope, and fed to a window discriminator. The window discriminator produced TTL pulses, each representing a single spike time, which were fed to a CED 1401*plus* (Cambridge Electronic Designs). The stimuli (see following text) were synchronized with the collection of the TTL pulses and peristimulus time histograms (PSTHs) were constructed with Spike2 for Windows software (Cambridge Electronic Designs).

Cells in LM are easily identifiable based on their direction-selective responses to largefield visual stimuli (e.g., Fu et al. 1998a,b; Winterson and Brauth 1985; Wylie and Frost 1996). Direction selectivity was initially assessed by moving a large ($\sim$90 $\times$ 90°) handheld stimulus (consisting of black bars, dots, and squiggles on a white background) in various directions in the contralateral visual field. Once a responsive cell was isolated, a directional tuning curve was obtained using high contrast sine wave gratings of an effective SF and TF. The directional tuning curves were done with either 15 or 22.5° increments. Each sweep consisted of 4 s of motion in one direction, a 3 s pause, 4 s of motion in the opposite direction, followed by a 3 s pause. The directions were presented randomly, and firing rates were averaged over three to five sweeps. Subsequent to establishing the direction preference, the spatiotemporal properties were determined by presenting high contrast gratings in the preferred and anti-preferred directions. For the majority of cells, we presented several different SFs (in the range of 0.015–2 cpd) at several different TFs (in the range of 0.15–16 Hz). For most cells, the standard stimulus protocol consisted of six SFs (0.031, 0.063, 0.125, 0.25, 0.5, and 1 cpd) presented at six TFs (0.031, 0.125, 0.5, 2, 8, and 16 Hz). Each sweep consisted of 4–5 s motion in the preferred direction, a 3–5 s pause, 4–5 s of motion in the anti-preferred direction, followed by a 3–5 s pause. The different stimuli were presented randomly, and firing rates were averaged from at least three sweeps. Contour plots of the mean firing rate in the spatiotemporal domain were made using Sigma Plot. The peak firing rate in the contour plot was used to assign the preferred SF/TF combination for each neuron. There are limitations to this procedure for assigning a neuron's spatiotemporal preference. In particular, with the lower TFs used (0.031 and 0.125 Hz) much less than one cycle of motion occurs in the 4–5 s epoch. Because of this, for some cells we presented the low TF stimuli for longer durations such that at least two cycles occurred (see following text, Fig. 6).

The drifting gratings were produced using a visual stimulus generator (VSG Three, Cambridge Research Services) and displayed in one of two ways. In some cases, the stimuli were displayed on a SONY multiscan 17se II monitor that was placed 35 cm from the bird. This stimulus, which was circular, measured $\sim$40° in diameter. In other instances the stimuli were backprojected by an InFocus LP750 data projector onto a tangent screen placed 50 cm from the bird. The circular stimulus measured $\sim$75° in diameter. The receptive fields of LM neurons are quite large, often as large as the entire contralateral hemifield. The borders of a receptive field are rather difficult to define, but a hot-spot is present near the center (Fu et al. 1998a,b). The monitor or screen was always centered at the hot spot of the receptive field. The location of the receptive field was qualitatively noted as frontal, lateral (i.e., at the inter-aural axis), or midway between these two positions.

Histology

In some cases, when the tungsten microelectrodes were used, electrolytic lesions were made with a stimulator (Grass Medical Instruments S-48) and constant current unit (Grass; 30 μA, 10 s, electrode positive). At the end of the experiment, all animals were given a lethal dose of pentabarbitol sodium (100 mg/kg ip) and immediately perfused with saline followed by 4% para-formaldehyde. The brains were extracted, postfixed for several hours (4% para-formaldehyde with 20% sucrose) and then left in 30% sucrose for $\geq$24 h. Using a microtome, frozen sections (45 μm thick in the coronal plane) through the pretectum were collected. The sections were mounted onto gelatin coated slides, dried, counterstained with neutral red, and coverslipped with Permount. Light microscopy was used to localize electrode tracts and the lesion sites.

RESULTS

Direction selectivity

We examined the responses of 35 pretectal cells to largefield drifting sine wave gratings of various SFs and TFs. Polar plots showing direction tuning curves of representative LM neurons are shown in Fig. 1. Most neurons, although broadly tuned, were excited in response to motion in a particular direction ("preferred" direction) and inhibited below the spontaneous rate in response to motion in the (approximately) opposite direction (anti-preferred direction). Of the 35 cells, 30 behaved in this manner (see Fig. 1, *A–E*). Of the other five cells, three showed the excitation to motion in the preferred direction but were either unaffected by stimuli moving in the anti-preferred direction or showed a small amount of excitation to motion in the anti-preferred direction (i.e., there was no inhibitory portion of the tuning curve; Figs. 1*F* and 6). Shown in Fig. 1*H*, one neuron showed strong excitation in response to motion in all directions. Fu et al. (1998a,b) have dubbed these as "omni-directional" neurons. However, this neuron was not found among the direction-selective cells (see DISCUSSION). The other neuron, shown in Fig. 1*G*, had a bi-directional tuning curve (Fu et al. 1998a,b). This neuron was excited by gratings moving in both the forward (temporal to nasal) and backward directions, although there was a slight preference for forward motion. Two tuning curves are shown for this neuron, in response to stimuli of either high (0.5 cpd) or low (0.0625 cpd) SF drifting at 2 Hz. For this cell, gratings of higher TF moving in the anti-preferred direction did result in inhibition of the firing rate below the spontaneous level (see following text and DISCUSSION).

A neuron's direction preference was assigned by calculating the maximum of the best cosine fit to the tuning curve. In Fig. 2 the direction preferences of the 33 direction-selective LM neurons (i.e., excluding the omni-directional and the bi-directional neurons) are plotted as unit vectors in polar coordinates. Note that there is an obvious clustering into four groups. Seventeen (53%), 5 (15%), 5 (15%), and 6 (18%) neurons preferred forward, backward, downward, and upward motion, respectively.

Spatiotemporal properties

We obtained contour plots of the spatiotemporal tuning in response to sine wave gratings moving in both the preferred and anti-preferred directions. Because, for most neurons, largefield motion in the preferred direction elicits excitation and

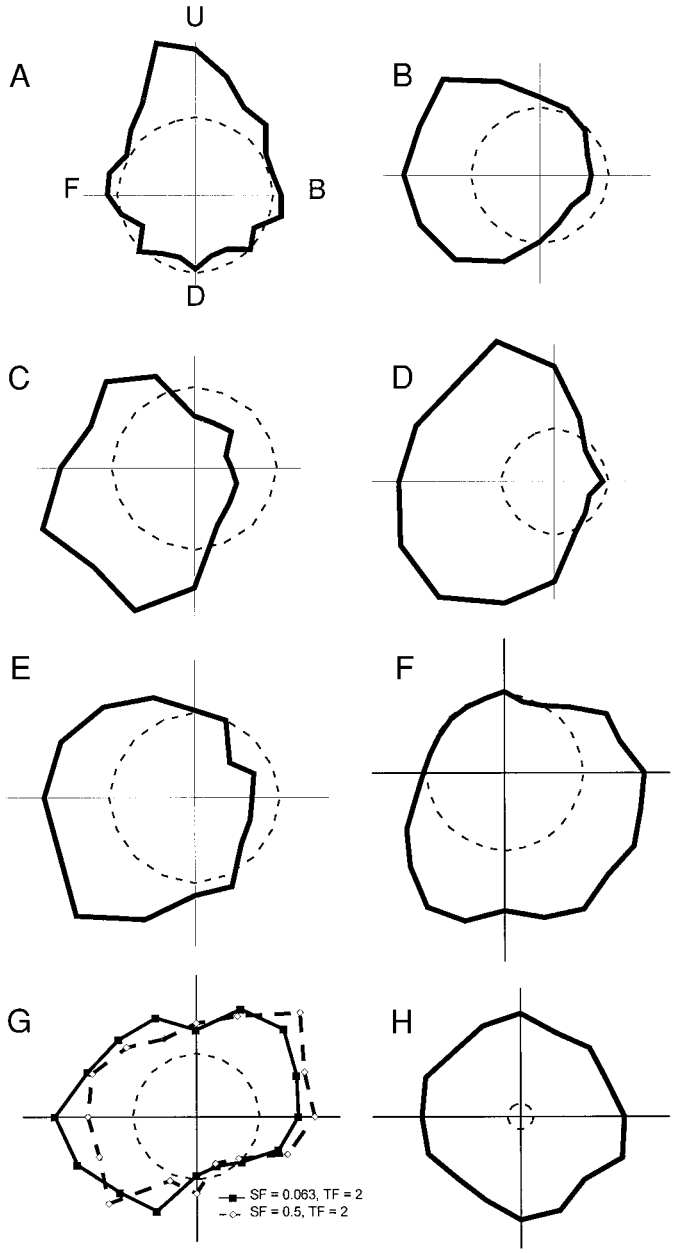

FIG. 1. Directional tuning curves of neurons in the pretectal nucleus lentiformis mesencephali (LM). Firing rate (normalized) is plotted as a function of the direction of grating motion in polar coordinates. Two tuning curves are shown for different SFs for the neuron in *G*. The broken circles represent the spontaneous firing rates. U, D, B, and F represent upward, downward, forward (temporal to nasal), and backward motion, respectively. See text for details.

motion in the anti-preferred direction elicits inhibition, we refer to these as excitatory response plots (ER plots) and inhibitory response plots (IR plots), respectively. Thirty-one of the 35 LM neurons showed both the excitatory and inhibitory responses (Fig. 1, *A–E*), whereas 2 showed only the ER (Fig. 1*F*), and there was no IR for the omni-directional neuron. Thus we obtained 35 ER plots and 31 IR plots of spatiotemporal tuning.

Figs. 3 and 4 show ER and IR plots of representative LM neurons. [Fig. 3 shows neurons that had fast ERs whereas Fig. 4 shows neurons that had slow ERs (see following text).] For the majority of contour plots, there was a single peak in the spatiotemporal domain. In some cases the peaks were quite sharp. For example, the ER plot for the LM cell in Fig. 3*B* shows a single peak at low SFs and high TFs. Relatively sharp singular peaks are also apparent in the ER plots shown in Figs. 4, *A* and *C*, and 3*A*, and the IR plots in Fig. 3, *A–C*. In other cases, contour plots exhibited a broad peak, as in the ER plots in Figs. 3*C* and 4*B* and the IR plots in Figs. 3*D* and 4, *A* and *B*.

In some contour plots there were clearly multiple peaks. For example, the ER plot in Fig. 3*D* contains two clear peaks. The primary peak was at 0.062 cpd/16 Hz [45 spikes/s above the spontaneous rate (SR)], but there was a secondary peak at 0.5 cpd/1 Hz (40 spikes/s above SR). Similarly, the ER plot of the LM neuron shown in Fig. 4*D* also contains two peaks (the peak at 2 cpd/0.5 Hz was the larger). In Fig. 4*C*, there are two peaks in the IR, but one was much larger. The primary peak was at 1 cpd/0.5 Hz (25 spikes/s below SR), and the smaller secondary peak was at low SFs and high TFs (5 spikes/s below SR). The neuron in Fig. 4*D* also showed two peaks in the IR plot. Of the 35 ER plots, 11 showed multiple (2 or 3) peaks. Of the 31 IR plots, 6 showed multiple peaks.

The ER of the bi-directional neuron shown in Fig. 1*G* had two peaks: one at 0.5 cpd/2 Hz, and the other at 0.625 cpd/2 Hz. Although this was not routinely done, directional tuning curves were assessed with both low SF and high SF gratings. Note that the directional tuning is similar for both SFs.

Bi-directional IR plots

In some IR plots, it was apparent that there were zones of inhibition and excitation. An example of this is shown in Fig. 3*D*. This cell showed a broad inhibitory peak for the lower SFs. However, gratings of high SFs and mid-high TFs, but still moving in the anti-preferred direction, caused excitation. This is particularly salient in the bottom PSTH shown on the *right* in Fig. 3*D*. (The symbols accompanying the PSTHs correspond to the symbols indicating locations on the contour plot.) In the top two PSTHs, one can see that the cell was silenced during the period of time that the grating was drifting in the anti-preferred direction (backward). However, a grating of 0.5

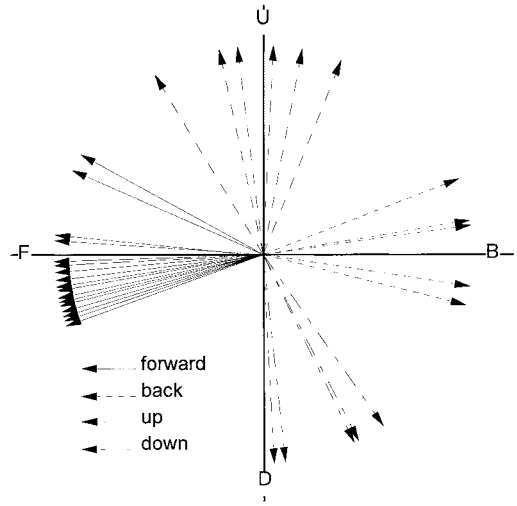

FIG. 2. Direction preferences of neurons in the nucleus LM. The arrows are unit vectors representing the preffered direction of LM neurons as calculated from the best fit cosines to the tuning curves. Note the tight clustering of the forward (temporal to nasal) selective neurons.

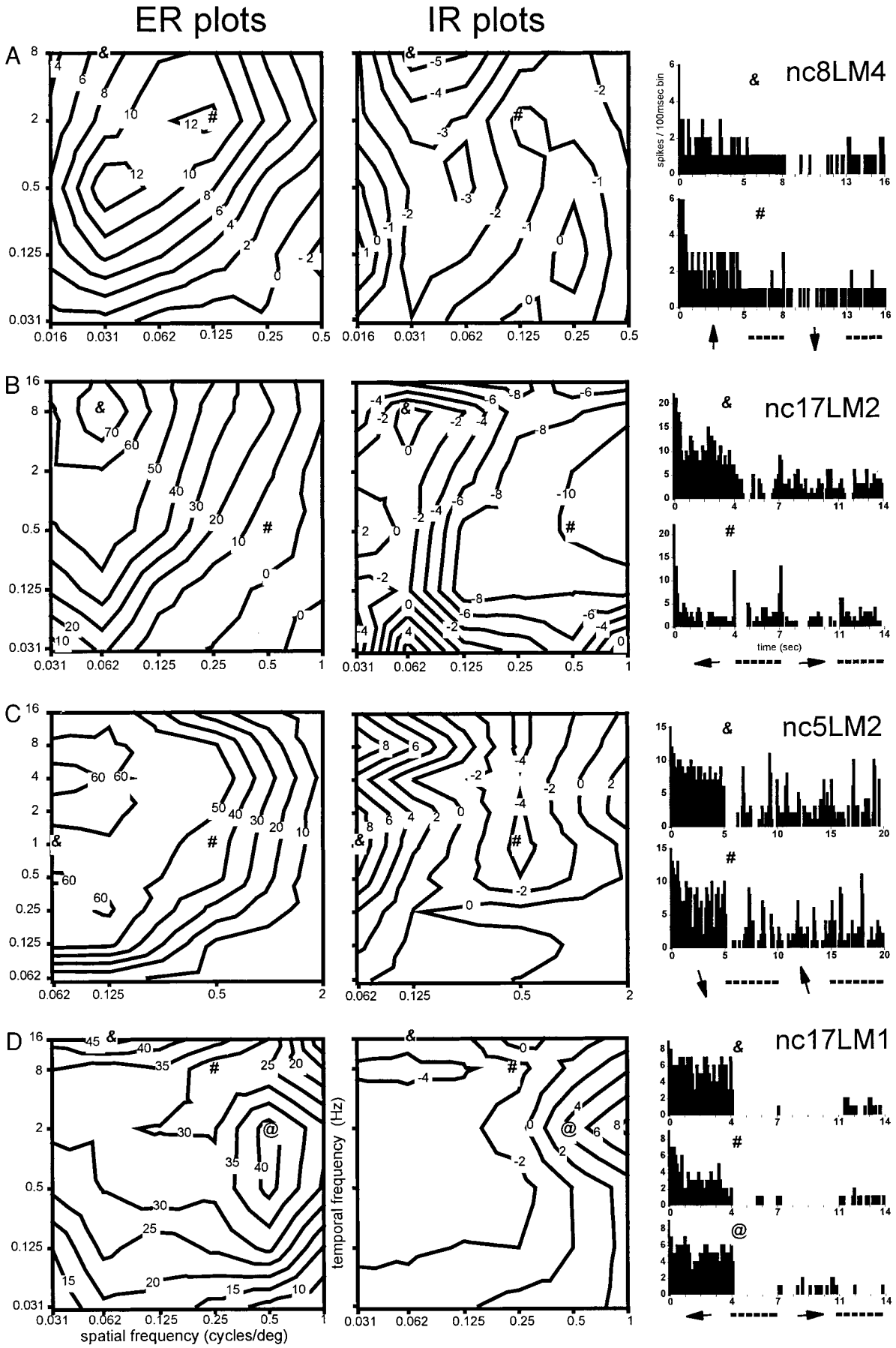
ER plots
IR plots
A
B
C
D
nc8LM4
nc17LM2
nc5LM2
nc17LM1
spikes / 100msec bin
time (sec)
temporal frequency (Hz)
spatial frequency (cycles/deg)

cpd/2 Hz drifting in the anti-preferred direction caused a small excitatory response. That is, this cell was excited in response to gratings of high SF and mid-high TF drifting in both the forward and backward directions. Another example of this bi-directional response to stimuli moving in the anti-preferred direction can be seen in Fig. 3*C*, but in this case, the excitatory region of in the IR plot was at low SFs (see also Fig. 4*B*). In total, the IR plots of 10 LM neurons showed this property. [The neuron with the bi-directional tuning curve (Fig. 1*G*) was one of these 10.] There was a tendency for this excitation peak in the IR to occur for stimuli of high SFs and low TFs or low SFs and high TFs. Similarly, two of the ER plots of LM neurons showed a weak inhibitory zone.

Independence of excitation and inhibition

For a given cell, we expected that the ER and IR plots would be identical. Although this was the case for some cells, this was not the norm. For example, for the LM neuron shown in Fig. 3*B*, the peak in the ER plot was at low SFs and high TFs, whereas the peak in the IR plot was at high SFs and mid-TFs. Likewise, in Fig. 4, *A* and *B*, the cells were maximally excited by high SF/mid-TF gratings drifting in the preferred direction but were maximally inhibited by low SF/high TF gratings drifting in the anti-preferred direction. In fact, for none of the eight cells shown in Figs. 3 and 4 did the ER plot show a similar response profile to the IR plot. Of the 31 LM neurons for which we obtained both ER and IR plots, 25 had markedly different spatiotemporal response profiles for the ER and IR.

Slow and fast responses

In Fig. 5 the locations of the response maxima are shown for the ER and IR plots of LM neurons. For those contour plots in which there were multiple peaks, the location of the primary peak was plotted. ER and IR plots with multiple maxima of equal size were excluded from this analysis as was the IR of one LM neuron that had an extremely broad plateau. In Fig. 5*A*, the peaks from the ER plots are shown. A cluster analysis using Ward's method with squared-Euclidean distance measures clearly revealed the two clusters shown in Fig. 5*A*. A discriminate analysis revealed that the groups were completely nonoverlapping. The first group (●) preferred low-mid SFs (0.031–0.25 cpd) and mid-high TFs (0.5–16 Hz). The second group (○) preferred mid-high SFs (0.3–2 cpd) and low-mid TFs (0.125–2 Hz). We refer to these groups as fast and slow neurons, respectively (velocity = TF/SF). The average SF, TF, and velocity of the fast neurons were 0.097 cpd, 2.88 Hz, and 29.2°/s, respectively. The average SF, TF, and velocity of the slow neurons were 0.67 cpd, 0.55 Hz, and 0.82°/s, respectively. (All values were first transformed to the natural log, the average was calculated, and then the inverse transformation was performed.)

Figure 5*B* show locations of the peaks from the IR plots. Unlike the ERs, the locations of the peak IRs do not exhibit any obvious clustering in the spatiotemporal domain. Although many of the peaks fell in the slow (high SF/low TF) and fast (low SF/high TF) regions, there were also several peaks in the high SF/high TF quadrant. (However, note that there is still an overall negative correlation between SF and TF.)

In Fig. 5, *right*, the same data are plotted as that on the *left*, but the direction preference is also indicated. There are a couple things to note. First, with respect to the ER plots, all but one of the slow cells preferred forward motion. Some cells that preferred forward motion had fast ERs, as did most of the LM cells that preferred up, down, and backward motion. Second, for the IR plots, there was a tendency for those cells with IR peaks in the lower TF range to prefer forward motion.

Examples of fast and slow LM neurons are shown in Figs. 3 and 4, respectively. We would like to emphasize two things about this classification. First, the designation of a neuron as fast or slow refers only to the ER. For example, the ER plot of LM cell in Fig. 3*B* had a peak in the fast region, but the peak for the IR was in the slow region. The peak ER for the cell shown in Fig. 4*A* was in the slow region, but the peak IR was in the fast region. Second, for neurons with multiple peaks in the ER, the designation of a neuron as fast or slow refers to the primary peak. The cell shown in Fig. 3*D* had peak ERs in both the fast and slow regions, although the former was slightly larger. Likewise the ER plot of the cell shown in Fig. 4*D* showed maxima in both the fast and slow region, although the peak in the slow region was slightly larger. This was generally the case for the ER (and IR) plots with multiple peaks: there were maxima in both the slow and fast regions.

Transients and temporal effects

Figure 6 shows PSTHs of the responses of an LM neuron to gratings drifting in the preferred (up) and anti-preferred (down) directions. In Fig. 6*A*, the responses of the neuron to 36 combinations of SF (abscissa) and TF (ordinate) are shown. Each PSTH is for a single sweep, where each sweep consisted of 4 s motion in the preferred direction (upward motion, —), followed by a 3 s pause, followed by 4 s of motion in the anti-preferred direction (downward motion, - - -). Note that this cell showed strong excitation to motion in the preferred direction and a small amount of excitation to motion in the anti-preferred direction. In Fig. 6*B*, PSTHs show the responses for the same cell to drifting gratings of 0.125 Hz at three different SFs. Each sweep consisted of 16 s of motion in the preferred, followed by a 3 s pause, followed by 16 s of motion in the anti-preferred direction. That is, there were two complete cycles of motion. This figure is shown to indicate some of the limitations with our procedure. More so than any other cell, this cell showed dramatic transient and temporal effects in the PSTHs. The response to motion in the preferred direction

FIG. 3. Spatiotemporal tuning of fast neurons in the pretectal nucleus LM. Contour plots of the responses of 4 LM neurons to gratings of varying spatial frequency (SF, abscissa) and temporal frequency (TF, ordinate) drifting in the preferred [excitatory response (ER) plots] and anti-preferred [inhibitory response (IR) plots] directions are shown. The scale on the iso-contour lines represents the firing rate (spikes/s) above (+) or below (−) the spontaneous rate. To the right of the contour plots, 2 or 3 peristimulus time histograms (PSTHs) show individual sweeps for a particular SF and TF. The particular SF and TF are indicated by the corresponding symbols (&, @, #) on the PSTH and the contour plot. For each sweep there was 4–5 s of motion in the preferred direction (indicated by the orientation of the arrow; left = forward), followed by a 3–5 s pause (i.e., a stationary grating; - - -), followed by 4–5 s of motion in the anti-preferred direction, followed by a 3–5 s pause.

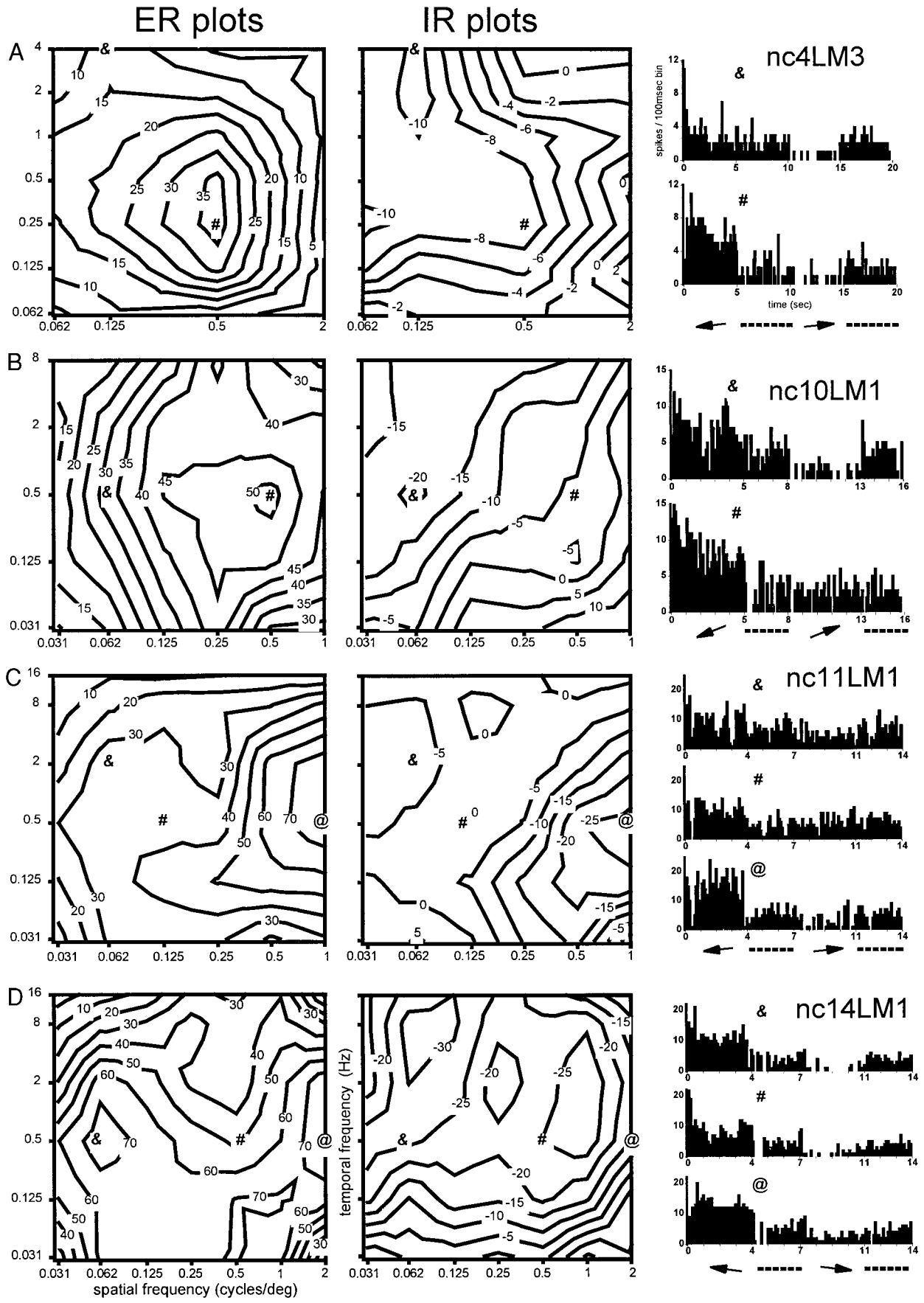

FIG. 4. Spatiotemporal tuning of slow neurons in the pretectal nucleus LM. See legend for Fig. 3 for additional details.

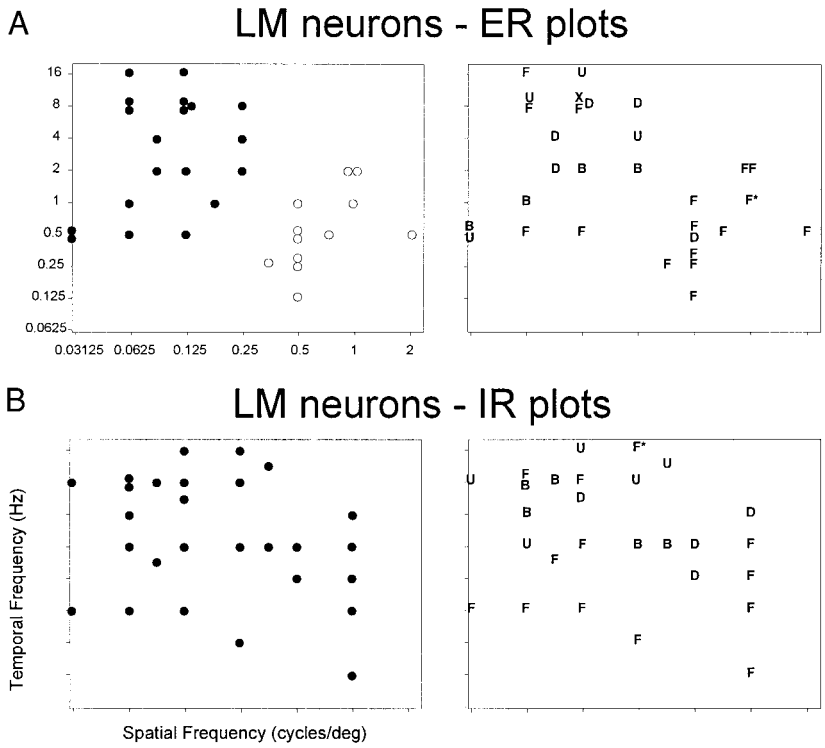

FIG. 5. Locations of the peak excitatory and inhibitory responses in the spatiotemporal domain for neurons in LM. *A* and *B*: the locations of the peaks are shown for the ER plots and the IR plots. Included in this analysis are ER and IR plots that showed single peaks as well as those that showed multiple peaks where there was a clear primary peak. (The locations of the primary peaks, but not the secondary peaks, are plotted.) *A*: ●, the group of fast ERs; ○, the group of slow ERs. *Right*: the same data are plotted, but the locations are indicated with a letter corresponding to the preferred direction of the cell. ×, the omni-directional cell (Fig. 1*H*); F*, the bi-directional cell (Fig. 1*G*). Note that for the IR plots (responses to motion in the anti-preferred direction), the *preferred* direction of the cell is indicated.

consisted of an onset transient, followed by a steady-state response. In response to some gratings, there was also an offset transient (e.g., 0.03 cpd/0.12 Hz), and onset and offset transients to motion in the anti-preferred direction (e.g., 0.25 cpd/0.12 Hz). The asterisk (*) indicates the peak excitatory response in the spatiotemporal domain (0.125 cpd/16 Hz) based on the average firing rate over the 4-s epoch. This encompasses the steady-state and transient responses. Note however, that the largest onset transient occurred in response to 0.25 cpd/2 Hz. The data in Fig. 6*B* indicate another possible shortcoming of our standard protocol. For the two lowest TFs used, less than one cycle of motion occurred during the 4-s epoch. When a 16-s epoch was used for stimuli drifting at 0.125 Hz (i.e., 2 complete cycles), other temporal effects were observed at some SFs. The PSTH in response to the lowest SF grating (0.03 cpd) clearly shows that the response to motion in both the preferred and anti-preferred directions was modulated at the TF of the stimulus. This TF modulation was not apparent in the response to the 0.125-cpd grating, which had a higher average firing rate. The response to the 0.5-cpd grating was modulated in the range of 0.5–0.6 Hz. Thus the standard protocol that we used, which limited the motion to 4- or 5-s epochs, would not necessarily capture all the temporal effects and might misrepresent the firing rate. For this neuron, the average firing rate to a 0.03 cpd/0.12 Hz grating was 8.35 spikes/s over the 4-s epoch, but 14.96 spikes/s over the 16-s epoch. This translates to an 80% increase but only a 6% increase relative to the maximal firing rate to the preferred SF/TF combination (0.125 cpd/16 Hz; 115 spikes/s). The difference was not as marked for the other two stimulus conditions shown in Fig. 6*B*. In response to a 0.125-cpd/0.12 Hz grating, the average firing rate was 55 spikes/s over the 4-s epoch and 45 spikes/s over the 16-s epoch. In response to a 0.5-cpd/0.12 Hz grating, the average firing rate was 21.35 spikes/s over the 4-s epoch and 19.86 spikes/s over the 16-s epoch. For five neurons (2 fast and 3 slow neurons), we tested the responses to the lower TF (0.12 and 0.03 Hz) gratings using the standard protocol and longer epochs that allowed two complete cycles of motion in each direction. Although the average firing rates over the two conditions were sometimes different, there were no changes with respect to the shapes of the contour plots or the location of the peaks in the contour plots.

Tuning for temporal frequency or velocity?

From the contour plots, it is easy to see if a cell is tuned to TF or velocity. Cells tuned to velocity have elliptical peaks and iso-contour lines that are oriented diagonally with a slope of 1. Cells tuned to TF have contour plots that are symmetrical about a horizontal line through the peak. For example, the ER plot of the LM cell in Fig. 3*A* showed velocity tuning. The elliptical peak and iso-contour lines are oriented diagonally with a slope of ~1. In Fig. 7*A*, the responses of this cell are shown as a function of velocity (*left*) and TF (*right*) for each SF tested. Responses to stimuli drifting in the preferred and anti-preferred directions are represented by ●, ▼, ■, ◆, ▲, ⬣ and ○, ▽, □, ◇, △, ⬡, respectively. To stimuli moving in the preferred direction, a peak response occurred at ~10°/s for most SFs tested. In Fig. 7*A*, *right*, where the response is plotted as a function of TF, there is not a common peak for all the SFs tested. However, responses tuned to velocity were uncommon (2 ER plots, 1 IR plots). More cells seemed to be tuned to a particular TF. For example, the ER of the LM cell in Fig. 7*B* showed a peak at 0.5–2 Hz for each SF tested. Similarly, the IR of the cell shown in Fig. 7*A* was tuned to higher TFs and

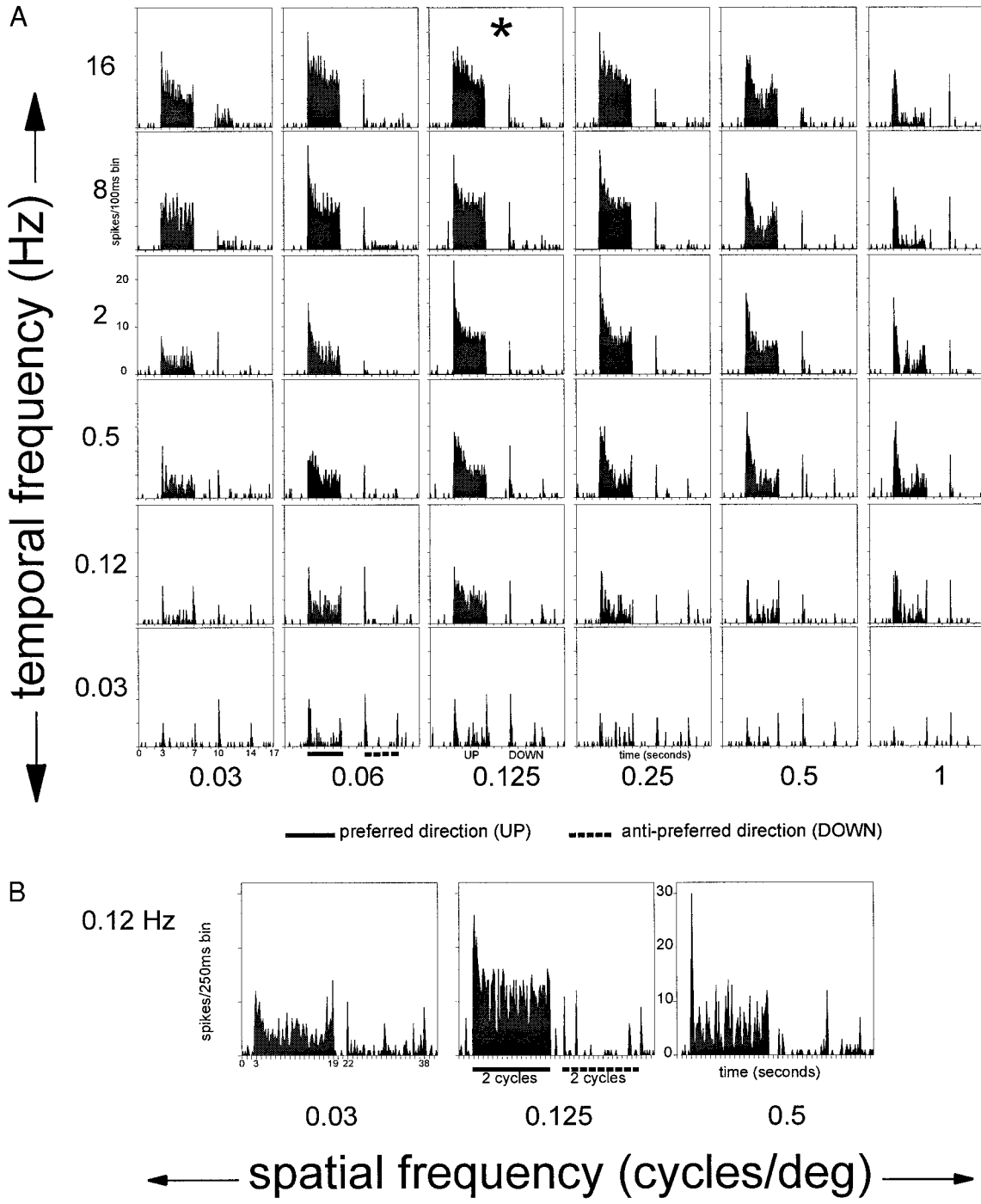

FIG. 6. Responses of a neuron in LM to drifting gratings of varying SF and TF. *A*: PSTHs show the responses of the neurons to 36 combinations of SF (abscissa) and TF (ordinate). Single sweeps are shown, where each sweep consisted of 4 s motion in the preferred direction (upward motion, —), followed by a 3-s pause, followed by 4 s of motion in the anti-preferred direction (downward motion, - - -). Note that the grid is not scaled. *, the peak excitatory response in the spatiotemporal domain based on the average firing rate over the 4-s epoch. *B*: PSTHs show the responses (for the same cell) to drifting gratings of 0.125 Hz at 3 different SFs. Each sweep consisted of 16 s of motion in the preferred direction (i.e., 2 complete cycles), followed by a 3-s pause, followed by 16 s of motion in the anti-preferred direction. See text for details.

the IR for the cell in Fig. 7*C* was tuned to 0.5–2 Hz. (The IR plot for this cell is shown in Fig. 4*D*.) The ERs of 14 LM neurons were reasonably well tuned to TF as were the IRs of 12 cells.

Many responses, including most of those that showed multiple peaks in the contour plots, could not be described as tuned to either a particular velocity or TF. For example, the ER for the cell shown in Fig. 7*C* was tuned to mid-TFs for stimuli of high and low SF, and low TFs for stimuli of mid-SFs. Likewise the IR in Fig. 7*B* was tuned to neither TF nor velocity (see also the ER plots in Figs. 3*D* and 4*C* and the IR plots in Figs. 3*B* and 4, *A* and *C*).

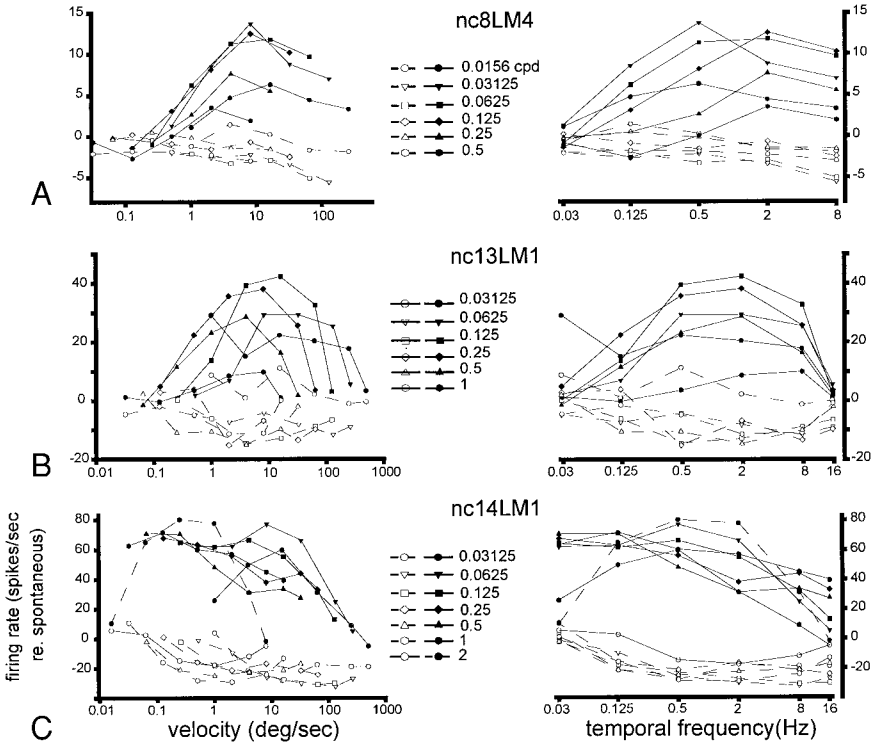

FIG. 7. Velocity and temporal frequency tuning of neurons in the pretectal nucleus LM. *Left*: average firing rate [spikes/s above (+) or below (−) the spontaneous rate (SR)] is plotted as a function of velocity (°/s) for each SF used. *Right*: the same data are plotted, but as a function of TF (Hz). ●, ▼, ■, ▲, ◆, ● and ○, ▽, □, △, ◇, ○, the responses to gratings moving in the preferred and anti-preferred directions, respectively. The neurons in *A* and *C* correspond to those in Figs. 3*A* and 4*D*, respectively. See text for details.

Histological results

For eight neurons the recording sites were localized with electrolytic lesions. In Fig. 8 the lesion sites are collapsed onto two coronal sections through the pretectum. We have used the nomenclature for the pigeon pretectum as established by Gamlin and Cohen (1988). All eight lesions were found in the LM, either in the medial or lateral subnuclei (LMm, LMl; 4 lesions each). There was no obvious anatomical separation of cells with respect to either direction preference or spatiotemporal properties (fast/slow), although the size of our sample is insufficient in this regard.

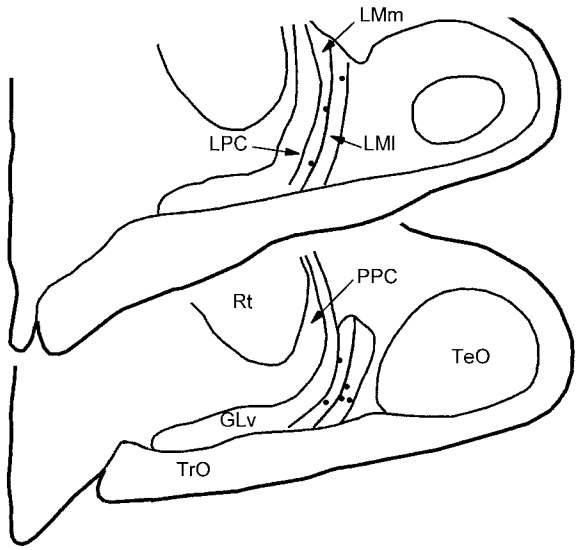

FIG. 8. Location of directionally selective units in the pretectum. Two coronal sections through the pretectum are shown (top = caudal) indicating the locations (●) of 8 recording sites marked by electrolytic lesions. The nomenclature of Gamlin and Cohen (1988) is used. The LM consists of medial and lateral subnuclei (LMm, LMl). LMm is bordered medially by the nucleus laminaris precommisuralis (LPC). The nucleus principalis precommisuralis (PPC) resides between the LPC and the nucleus rotundus (Rt). Note that all the marking lesions were located in the LM. GLv, nucleus geniculatus lateralis, pars ventralis; TeO, optic tectum; TrO, tractus opticus.

DISCUSSION

In the present study, we examined the responses of neurons in pigeon pretectum to largefield drifting sine wave gratings varying in spatial and temporal frequency. Although we did not leave marking lesions at all of the recording sites, all of the lesions were located in LM (see Fig. 8). However, this does not preclude the possibility that some of the other visually responsive units were located in other areas of the pretectum (Winterson and Brauth 1985).

As previously reported in numerous other studies in several species, pretectal neurons exhibit directional selectivity in response to such largefield stimuli (mammals: Collewijn 1975a,b; Hoffmann and Distler 1989; Hoffman and Schoppmann 1975, 1981; Hoffmann et al. 1988; Ibbotson et al. 1994; Mustari and Fuchs 1990; Volchan et al. 1989; birds: Fu et al. 1998a,b; Winterson and Brauth 1985; Wylie and Frost 1996; amphibians: Fite et al. 1989; Katte and Hoffmann 1980; Li et al. 1996; Manteuffel 1984). Unlike previous studies, we used drifting sine wave gratings as stimuli. We are aware of only two previous studies that used such stimuli: Wolf-Oberhollenzer and Kirschfeld (1994) in a study of neurons in pigeon nBOR, and Ibbotson et al. (1994) in a study of neurons in the wallaby NOT, the mammalian homologue of the LM. The bulk of the discussion will focus on comparing the results of the present study with those previous studies.

Independence of excitation and inhibition

One of the surprising findings of the present study was that spatiotemporal properties of the inhibitory and excitatory re-

sponses for a given cell were often quite different. This was that case for 25/31 LM neurons. This was not noted in the study of the NOT by Ibbotson et al. (1994), but they only showed contour plots for stimuli moving in the preferred direction. However, one figure (Fig. 7, p. 2933) clearly shows a NOT cell for which there was a difference in the preferred TF to stimuli drifting in the preferred versus anti-preferred directions. The independence of excitatory and inhibitory responses of AOS and pretectal neurons has been noted with respect to other properties. First, with respect to direction tuning, the preferred and anti-preferred directions of AOS neurons are often not 180° apart (e.g., Burns and Wallman 1981; Rosenberg and Ariel 1998; Soodak and Simpson 1988; Wylie and Frost 1990). Second, it has been noted that the excitatory and inhibitory receptive fields of an individual LM or nBOR neuron may differ with respect to their size and position (Fu et al. 1998a; Wylie and Frost 1990; Zhang et al. 1999). Together these findings suggest that the inhibitory and excitatory inputs to direction-selective LM neurons arise from different inputs. Perhaps the excitatory input is of retinal origin (Kogo et al. 1998), whereas the inhibitory inputs are extra-retinal (Brecha et al. 1980; Miceli et al. 1979).

Comparison with previous studies of the pigeon LM

Previous studies have examined the responses of pigeon LM neurons to largefield stimuli that contain multiple SF components [random dot patterns, checkerboards and/or square wave gratings (Fu et al. 1998a,b; Winterson and Brauth 1985; Wylie and Frost 1996)]. As with these previous studies, we found that most LM neurons prefer largefield stimuli moving forward in the contralateral visual field, whereas fewer prefer upward, downward, or backward motion (Fu et al. 1998a,b; Winterson and Brauth 1985; Wylie and Frost 1996). With respect to fast and slow neurons, our findings are in strong agreement with Winterson and Brauth (1985). They described slow neurons that preferred stimuli moving at <1.0°/s and fast neurons that preferred velocities in the range of 3.3–80°/s. These data are confirmed by the present study: with respect to the ER plots, we describe slow neurons (0.25–2°/s) and fast neurons (4–256°/s). Further, we show that velocity is not the correct referent for the vast majority of cells: slow neurons preferred high SF/low TF gratings and fast neurons preferred low SF/high TF gratings. In their sample, Winterson and Brauth (1985) noted that most (8/9) of the slow neurons preferred forward motion, whereas the fast neurons preferred either forward, backward, upward, or downward motion. This is essentially identical to what we found: 11/12 slow neurons were forward cells, whereas the fast cells included forward, backward, downward and upward cells. Stated another way, there were fast and slow forward cells in LM, in addition to fast cells that preferred upward, downward, and backward motion.

The results of the present study are, for the most part, in agreement with the findings of Fu et al. (1998b). Using square wave gratings and other largefield moving stimuli, they described three types of neurons: uni-directional cells (74%) responded to motion in a particular direction, were inhibited by motion in the opposite direction, and preferred slow velocities (0.1–11°/s); omni-directional neurons (9%) responded equally well to motion in all directional and preferred fast velocities (34–67 deg/s); and bi-directional neurons (17%) had bi-lobed tuning and were excited by motion in two, approximately opposite, directions. The results of the present study are different from these of Fu et al. (1998b) on several accounts. First, most (33/35) of the LM cells we recorded from would be classified as uni-directional, but these included fast and slow neurons. Fu et al. (1998b) did note within this group of unidirectional cells, the average preferred velocity of the forward cells was slower than that of the backward cells. Second, we did record from one omni-directional neuron that preferred low SFs and high TFs, but it was not found among the unidirectional cells. In subsequent experiments, when we encountered omni-directional neurons, we moved caudally to find the direction-selective cells. Although we have no supportive histology, we believe that the omni-directional cells may not reside in the LM but are located elsewhere in the pretectum [perhaps the nucleus laminaris precommissuralis (LPC), the nucleus principalis precommissuralis (PPC) or the tectal gray; Fig. 8; see Gamlin and Cohen 1988]. In their study of the LM, Winterson and Brauth (1985) did not report these omni-directional cells. Third, we also only encountered one of the bi-directional cells described by Fu et al. (1998b). However, we must emphasize that the cell showed either excitation or inhibition to gratings moving in the anti-preferred direction, dependent on the SF and TF. The directional tuning curve shown in Fig. 1*G* was not done with the appropriate SF and TF to elicit inhibition to stimuli moving in the anti-preferred direction. Thus it is possible that the bi-directional cells found by Fu et al. (1998b) were actually unidirectional cells, but the stimuli used did not contain the appropriate SF/TF combination in the range of the inhibitory peak. Recall that, in the present study, the IR plots of 32% of the LM neurons had zones of excitation and inhibition in response to stimuli moving in the anti-preferred direction. This is clearly illustrated by the cell in Fig. 3*D*: gratings of high SF/mid-TF moving in the anti-preferred direction excite the cell, whereas gratings of low SF/high TF inhibit the cell. For this cell, if directional tuning was established with stimuli containing low SFs, this cell would be classified as unidirectional, but if tested with high SFs the cell could be classified as bi-directional.

Finally, Fu et al. (1998b) concluded that LM neurons are essentially "edge detectors" (see also Zhang et al. 1999). That is, LM neurons require a sharp edge to elicit a maximal response. We find this hard to reconcile given that we recorded from many neurons that showed maximal responses to low SF sine wave gratings that are essentially bars with blurry edges. Moreover, in the initial open-loop stages of OKN and until the steady-state OKN is achieved (i.e., when the OKN gain is very low), any edges will be blurred (Ibbotson et al. 1994). We have closely examined the methods Fu et al. (1998b) used to reach this conclusion and offer an alternative explanation. They had an edge drift across a screen that subtended ~140°. Leading the edge, the stimulus was completely white, and trailing the edge the stimulus was completely black. They found that the neurons responded vigorously to a sharp edge, but the response was progressively reduced as the edge was progressively blurred by altering the spatial rate of luminance change at the border. However, note that such a stimulus is effectively an extremely low SF grating (~0.004 cpd) with progressively more power at higher SFs as the edge becomes progressively sharper. As we interpret their results, the progressively sharper edges simply had progressively more power at higher SFs.

That is, it is possible that the sharp edges had sufficient power in the range of SFs that the cell preferred, whereas the blurred edges did not.

Comparison with previous studies of nBOR

Like the LM, the nBOR is also involved in the analysis of optic flow and the generation of compensatory head and eye movements (Fite et al. 1979; Gioanni et al. 1983a). The major difference between the LM and nBOR is that most nBOR neurons prefer largefield stimuli moving upward, downward, or backward in the contralateral visual field, whereas few prefer forward motion (Burns and Wallman 1981; Gioanni et al. 1984; Wylie and Frost 1990; Zhang et al. 1999). Wolf-Oberhollenzer and Kirschfeld (1994) examined the responses of neurons in nBOR to drifting sine wave gratings, but they did not use as extensive a battery of stimuli as we used in the present study. They used TFs in the range of 0.1–10 Hz, but only four levels of SF in the range of 0.024–0.185 cpd. This is the lower half of the SF range we used. They noted that most nBOR neurons could not be described as velocity detectors. In fact only 1 of 15 (7%) neurons tested responded to stimulus velocity, whereas 7 (47%) were described as selective for a given TF at all SFs tested. This is strikingly similar to what we found for LM neurons. Collapsing across the ERs and IRs, 5% showed velocity selectivity, whereas ~40% showed similar TF response profiles for all SFs tested.

Because Wolf-Oberhollenzer and Kirschfeld (1994) did not use a more broad range of SFs, it is difficult to compare our results directly. Nonetheless they described two groups of nBOR neurons. The first group showed a single peak TF at ~0.2 Hz, although it is not stated if these neurons responded better to the higher SF used. In the present study, on average, the slow ERs of LM neurons preferred a TF of ~0.5 Hz. Wolf-Oberhollenzer and Kirschfeld (1994) did not report any neurons that had a single peak in the high TF region. The second group they described showed two peaks in the TF domain: one at 0.2 Hz and the other in the range of 1–7 Hz. Similarly, we described neurons with multiple peaks, most with one each in the low SF/high TF region and the high SF/low TF region. Although, Wolf-Oberhollenzer and Kirschfeld (1994) assumed that these neurons receive inputs from two types of motion detectors that have low-pass filters with differing time constants, we would add that the two types of detectors might also have different SF preferences.

Comparison with the spatiotemporal preferences of NOT neurons

Ibbotson et al. (1994) examined the spatiotemporal properties of neurons in the NOT of the wallaby using a broad range of SFs (0.063–2 cpd) and TFs (0.38–24.3 Hz). They found two groups of cells. Slow cells preferred high SFs (0.5–1.0 cpd) and low TFs (<1 Hz), whereas fast neurons preferred low SFs (0.1–0.5 cpd) and high TFs (>10 Hz). These findings are similar to the findings of the present study, but there were some differences. First, the slow NOT neurons were inhibited by low SF/high TF gratings moving in the preferred direction. We saw such bi-directional responses but in response to gratings moving in the anti-preferred direction. Second, all of the fast NOT neurons showed a secondary peak in the slow region. We did find neurons with peaks in both the fast and slow regions, but others with a single peak in the fast region. Third, the range of preferred SFs for the fast NOT neurons is higher than that of the fast ERs of LM neurons. Finally both the slow and fast NOT neurons in the wallaby are faster than their counterparts in the pigeon LM. This difference might be related to the differences that are seen in the properties of the OKN (see following text).

Function of fast and slow neurons

Ibbotson et al. (1994) provide an excellent discussion of the potential role of the slow and fast NOT neurons in the generation and maintenance of OKN. Immediately after the onset of an optokinetic stimulus, there is a 50- to 100-ms latent period before ocular following begins (e.g., Collewijn 1972). During this period, the retinal slip velocity (RSV) is high, and Ibbotson et al. (1994) suggest that the fast NOT neurons are responsible for initiating ocular following (the "direct" phase of OKN) (Cohen et al. 1977). Moreover, they suggest that the fast neurons are involved in the charging of the velocity storage mechanism ("indirect" phase of OKN) when stimulus speeds are high. Ibbotson et al. (1994) note that rapidly moving visual images become blurred, which is consistent with the fact that the fast NOT neurons respond best to low SFs. The slow NOT neurons do not become active until the RSV is low, and they continue to charge the velocity storage mechanism at these slow velocities. Finally, Ibbotson et al. (1994) suggested that omni-directional neurons in NOT inhibit direction-selective neurons in the early stages of saccades.

Gioanni and colleagues (Gioanni 1988; Gioanni et al. 1981) have provided a comprehensive description of the OKN and head-free OCR in pigeons. OKN in pigeons is different from that of frontal-eyed mammals in (at least) two respects. First, pigeons lack the direct phase of OKN, but they do possess a velocity storage mechanism (Gioanni 1988). This precludes the fast LM ERs in pigeon from a role in the direct component of OKN, as proposed for the fast NOT neurons. However, it is reasonable to imagine that the fast and slow LM neurons are involved in charging the velocity storage mechanism as proposed for the fast and slow NOT neurons. The second difference between the dynamics of the OKN in pigeons and frontal-eyed mammals is that, in pigeons, the gain of the OKN falls markedly as stimulus velocity increases beyond 20°/s (although the OCR gain remains high at 40°/s) (Gioanni 1988). In frontal-eyed mammals the gain of the OKN remains high beyond 60°/s (e.g., Lisberger et al. 1981). In the present study, the average preferred velocity of the fast LM neurons was ~20°/s: the point at which the OKN gain begins to decline in pigeons. The fast NOT neurons in the wallaby preferred higher TFs than the fast LM ERs, which is correlated with a higher OKN gain at faster velocities in frontal-eyed mammals.

We thank H. Lehmann for technical assistance, Dr. C. Varnhagen for help with the cluster analysis, and Dr. M. Dawson for help with the discriminate analysis.

This work was supported by funding from the Natural Sciences and Engineering Research Council of Canada to D.R.W. Wylie. N. A. Crowder was

supported by a summer studentship from the Alberta Heritage Foundation for Medical Research.

REFERENCES

BRECHA N, KARTEN HJ, AND HUNT SP. Projections of the nucleus of basal optic root in the pigeon: an autoradiographic and horseradish peroxidase study. *J Comp Neurol* 189: 615–670, 1980.

BURNS S AND WALLMAN J. Relation of single unit properties to the oculomotor function of the nucleus of the basal optic root (AOS) in chickens. *Exp Brain Res* 42: 171–180, 1981.

COHEN B, MATSUO V, AND RAPHAN T. Quantitative analysis of the velocity characteristics of optokinetic nystagmus and optokinetic after-nystagmus. *J Physiol (Lond)* 270: 321–344, 1977.

COLLEWIJN H. Latency and gain of the rabbit's optokinetic reactions to small movements. *Brain Res* 36: 59–70, 1972.

COLLEWIJN H. Direction-selective units in the rabbit's nucleus of the optic tract. *Brain Res* 100: 489–508, 1975a.

COLLEWIJN H. Oculomotor areas in the rabbit's midbrain and pretectum. *J Neurobiol* 6: 3–22, 1975b.

FAN TX, WEBER AE, PICKARD GE, FABER KM, AND ARIEL M. Visual responses and connectivity in the turtle pretectum. *J Neurophysiol* 73: 2507–2521, 1995.

FITE KV, KWEI-LEVY C, AND BENGSTON L. Neurophysiological investigation of the pretectal nucleus lentiformis mesencephali in *Rana pipiens. Brain Behav Evol* 34: 164–170, 1989.

FITE KV, REINER T, AND HUNT S. Optokinetic nystagmus and the accessory optic system of pigeon and turtle. *Brain Behav Evol* 16: 192–202, 1979.

FU YX, GAO HF, GUO MW, AND WANG SR. Receptive field properties of visual neurons in the avian nucleus lentiformis mesencephali. *Exp Brain Res* 118: 279–285, 1998a.

FU YX, XIAO Q, GAO HF, AND WANG SR. Stimulus features eliciting visual responses from neurons in the nucleus lentiformis mesencephali in pigeons. *Vis Neurosci* 15: 1079–1087, 1998b.

GAMLIN PDR AND COHEN DH. Projections of the retinorecipient pretectal nuclei in the pigeon (*Columba livia*). *J Comp Neurol* 269: 18–46, 1988.

GIBSON JJ. The visual perception of objective motion and subjective movement. *Psychol Rev* 61: 304–314, 1954.

GIOANNI H. Stabilizing gaze reflexes in the pigeon *(Columba livia)*. I. Horizontal and vertical optokinetic eye (OKN) and head (OCR) reflexes. *Exp Brain Res* 69: 567–582, 1988.

GIOANNI H, REY J, VILLALOBOS J, BOUYER JJ, AND GIOANNI Y. Optokinetic nystagmus in the pigeon (*Columba livia)*. I. Study in monocular and binocular vision. *Exp Brain Res* 44: 362–370, 1981.

GIOANNI H, REY J, VILLALOBOS J, AND DALBERA A. Single unit activity in the nucleus of the basal optic root (nBOR) during optokinetic, vestibular and visuo-vestibular stimulations in the alert pigeon (*Columba livia*). *Exp Brain Res* 57: 49–60, 1984.

GIOANNI H, REY J, VILLALOBOS J, RICHARD D, AND DALBERA A. Optokinetic nystagmus in the pigeon (*Columba livia*). II. Role of the pretectal nucleus of the accessory optic system. *Exp Brain Res* 50: 237–247, 1983a.

GIOANNI H, VILLALOBOS J, REY J, AND DALBERA A. Optokinetic nystagmus in the pigeon (*Columba livia*). III. Role of the nucleus ectomammilaris (nEM): interactions in the accessory optic system. *Exp Brain Res* 50: 248–258, 1983b.

GRASSE KL AND CYNADER MS. The accessory optic system in frontal-eyed animals. In: *Vision and Visual Dysfunction. The Neuronal Basis of Visual Function,* edited by Leventhal A. New York: MacMillan, 1990, vol. IV, p. 111–139.

HOFFMANN KP AND DISTLER C. Quantitative analysis of visual receptive fields of neurons in nucleus of the optic tract and dorsal terminal nucleus of the accessory optic tract in macaque monkey. *J Neurophysiol* 62: 416–428, 1989.

HOFFMANN KP, DISTLER C, ERICKSON RG, AND MADER W. Physiological and anatomical identification of the nucleus of the optic tract and dorsal terminal nucleus of the accessory optic tract in monkeys. *Exp Brain Res* 69: 635–644, 1988.

HOFFMANN KP AND SCHOPPMANN A. Retinal input to direction selective cells in the nucleus tractus opticus of the cat. *Brain Res* 99: 359–366, 1975.

HOFFMANN KP AND SCHOPPMANN A. A quantitative analysis of the direction-specific response of neurons in the cat's nucleus of the optic tract. *Exp Brain Res* 42: 146–157, 1981.

IBBOTSON MR, MARK RF, AND MADDESS TL. Spatiotemporal response properties of direction-selective neurons in the nucleus of the optic tract and the dorsal terminal nucleus of the wallaby *Macropus eugenii. J Neurophysiol* 72: 2927–2943, 1994.

KARTEN HJ AND HODOS W. *A Stereotaxic Atlas of the Brain of the Pigeon (Columba Livia).* Baltimore: Johns Hopkins Press, 1967.

KATTE O AND HOFFMAN KP. Direction specific neurons in the pretectum of the frog (*Rana esculenta*). *J Comp Physiol* 140: 53–57, 1980.

KOGO N, RUBIO DM, AND ARIEL M. Direciton-tuning of individual retinal inputs to the turtle accessory optic system. *J Neurosci* 18: 2673–2684, 1998.

LI Z, FITE KV, MONTGOMERY NM, AND WANG SR. Single-unit response to whole-field visual stimulation in the pretectum of *Rana pipiens. Neurosci Lett* 218: 193–197, 1996.

LISBERGER SG, MILES FA, OPTICAN LM, AND EIGHMY BB. Optokinetic response in monkey: underlying mechanisms and their sensitivity to long-term adaptive changes in the vestibuloocular reflex. *J Neurophysiol* 45: 869–890, 1981.

MANTEUFFEL G. Electrophysiology and anatomy of direction-specific pretectal units in Salamandra salamandra. *Exp Brain Res* 54: 415–425, 1984.

MICELI D, GIOANNI H, REPÉRANT J, AND PEYRICHOUX J. The avian visual wulst. I. An anatomical study of afferent and efferent pathways. In: *Neuronal Mechanisms of Behaviour in the Pigeon,* edited by Granda AM and Maxwell JH. New York: Plenum, 1979, p. 223–239.

MUSTARI MJ AND FUCHS AF. Discharge patterns of neurons in the pretectal nucleus of the optic tract (NOT) in the behaving primate. *J Neurophysiol* 64: 77–90, 1990.

ROSENBERG AF AND ARIEL M. Analysis of direction-tuning curves of neurons in the turtle's accessory optic system. *Exp Brain Res* 121: 361–370, 1998.

SIMPSON JI. The accessory optic system. *Annu Rev Neurosci* 7: 13–41, 1984.

SIMPSON JI, GIOLLI RA, AND BLANKS RHI. The pretectal nuclear complex and the accessory optic system. In: *Neuroanatomy of the Oculomotor System,* edited by Buttner-Ennever JA. Amsterdam: Elsevier, 1988, p. 335–364.

SOODAK RE AND SIMPSON JI. The accessory optic system of rabbit. I. Basic visual response properties. *J Neurophysiol* 60: 2055–2072, 1988.

VOLCHAN E, ROCHA-MIRANDA CE, PICANCO-DINIZ CW, ZINSMEISSER B, BERNARDES RF, AND FRANCA JG. Visual response properties of pretectal units in the nucleus of the optic tract of the opossum. *Exp Brain Res* 78: 380–386, 1989.

WINTERSON BJ AND BRAUTH SE. Direction-selective single units in the nucleus lentiformis mesencephali of the pigeon (*Columba livia*). *Exp Brain Res* 60: 215–226, 1985.

WOLF-OBERHOLLENZER F AND KIRSCHFELD K. Motion sensitivity in the nucleus of the basal optic root of the pigeon. *J Neurophysiol* 71: 1559–1573, 1994.

WYLIE DR AND FROST BJ. Visual response properties of neurons in the nucleus of the basal optic root of the pigeon: a quantitative analysis. *Exp Brain Res* 82: 327–336, 1990.

WYLIE DRW AND FROST BJ. The pigeon optokinetic system: visual input in extraocular muscle coordinates. *Vis Neurosci* 13: 945–953, 1996.

ZHANG T, FU Y-X, AND WANG S-R. Receptive field characteristics of neurons in the nucleus of the basal optic root in pigeons. *Neurosci* 91: 33–40, 1999.